

COMPARISON OF THE CONSERVATIVE AND A CONSISTENT APPROACH FOR THE COUPLING OF NON-MATCHING MESHES

Aukje de Boer, Alexander H. van Zuijlen and Hester Bijl

Department of Aerospace Engineering

Delft University of Technology

Kluyverweg 2, 2629 HT Delft, The Netherlands

e-mail: A.deBoer@tudelft.nl

Key words: Fluid-Structure Interaction, Partitioned Coupling, Non-matching Meshes, Coupling Schemes.

Abstract. *In fluid-structure interaction simulations the meshes at the fluid-structure interface usually do not match, because of the different mesh requirements for the flow and structure. The exchange of data over the discrete interface becomes then far from trivial. In this paper we investigate the difference in accuracy and efficiency between a conservative and a consistent coupling approach. This is done for an analytical test problem as well as a quasi-1D FSI problem, for different coupling methods found in literature. It is found that when the coupling method is based on a weak formulation of the coupling conditions the conservative approach is the best choice. For other coupling methods the consistent approach provides the best accuracy and efficiency, because the conservative approach results in unphysical oscillations in the pressure received by the structure and is therefore not consistent.*

1 INTRODUCTION

Many engineering applications involve fluid-structure interaction (FSI) phenomena and FSI simulations are crucial for an efficient and safe design. For instance light-weight airplanes, long span suspension bridges and modern wind turbines are susceptible to dynamic instability due to aeroelastic effects. Computers and numerical algorithms have significantly advanced over the last decade, such that the simulation of these problems has become feasible.

In FSI computations it is required that pressure loads are transmitted from the fluid side of the fluid-structure interface to the structural nodes on that interface. Also, once the motion of the structure has been determined, the motion of the fluid mesh points on the interface has to be imposed. In FSI simulations generating matching meshes at the fluid-structure interface is usually not desirable, because the flow generally requires a much

finer mesh than the structure. In addition, also different teams may take care of the different physical domains. This means that the discrete interface between the domains may not only be non-conforming, but there may also be gaps and/or overlaps between the meshes. The exchange of data over the discrete interface becomes then far from trivial. In Figure 1 a 2D example of a non-matching discrete interface between a flow and structure domain is shown. When the meshes are non-matching, an interpolation/projection step has to be carried out to enable transfer of information between the two domains. In literature different methods can be found to transfer data between non-matching meshes, such as nearest neighbour interpolation¹, projection methods^{2,3,4} and methods based on interpolation by splines^{5,6,7}.

The general opinion is that energy should be conserved over the interface leading to a conservative coupling approach⁸. This approach is based on the global conservation of virtual work over the interface, where one transformation matrix performs both the transfer of displacements and pressure loads between the two discrete interfaces. However, for a general coupling method this can lead to unphysical oscillations in the pressure forces received by the structure as is briefly mentioned by *Ahrem et al*⁹. Especially for flexible structures this can have a large negative influence on the accuracy of the solution.

Instead of using the same transformation matrix for both transferring the displacement and pressure loads over the interface, two different transformation matrices can be defined. This leads to a consistent coupling approach without unphysical oscillations in the pressure forces. However, conservation of energy over the interface is not guaranteed. For partitioned coupling techniques this does not have to be a problem, because in unsteady computations energy is generally not conserved due to errors caused by the coupling in the time integration. In general, when the error introduced by the information transfer is smaller than the discretization error, this error does not affect the stability and accuracy of the computation.

In this paper we investigate the difference in accuracy and efficiency between the conservative and consistent approach for the coupling methods described in *de Boer et al*¹⁰. First the consistent and conservative approach are presented followed by a short description of the different coupling methods. The difference in the interpolation properties between the two approaches is investigated using an analytical test problem. A simple quasi-1D FSI problem is used to investigate the performance of the methods in FSI computations.

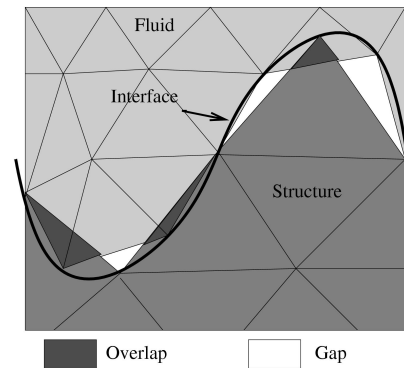


Figure 1: Non-matching meshes in 2D.

2 CONSISTENT AND CONSERVATIVE COUPLING APPROACH

The fluid and structure equations are usually coupled by the kinematic and dynamic boundary conditions at the interface which are given by

$$\mathbf{u}_f = \mathbf{u}_s \quad \text{on } \Gamma, \quad (1a)$$

$$p_s \mathbf{n}_s = p_f \mathbf{n}_f \quad \text{on } \Gamma, \quad (1b)$$

with $\mathbf{u}_{f,s}$ the displacement, $p_{f,s}$ the pressure or stress tensor and $\mathbf{n}_{f,s}$ the outward normal of the flow and structure interface, respectively. The continuous interface between the flow and structure is represented by Γ . The first of these two boundary equations expresses the compatibility between the displacement fields of the structure and the fluid at the fluid-structure interface. The second equation states that the tractions of the wet surface of the structure are in equilibrium with those on the fluid side.

Whichever coupling method is chosen to define the discrete form of these conditions, its outcome can be formulated as

$$\mathbf{U}_f = H_{sf} \mathbf{U}_s \quad (2a)$$

$$\mathbf{P}_s = H_{fs} \mathbf{P}_f, \quad (2b)$$

with H_{sf} and H_{fs} transformation matrices between the flow and structure interface and \mathbf{U} and \mathbf{P} are defined by the approximations

$$\mathbf{u}(\mathbf{x}) = \sum_{i=1}^{n^u} N^i(\mathbf{x}) \mathbf{U}_i, \quad p\mathbf{n}(\mathbf{x}) = \sum_{j=1}^{n^p} D^j(\mathbf{x}) \mathbf{P}_j, \quad (3)$$

where $n_{u,p}$ is the number of unknowns on the interface for the displacement and pressure, respectively, $N(\mathbf{x})$ a function depending on the discretization method used for the displacement (for example, a step function in the finite volume formulation or the basis function in the finite element formulation) and $D(\mathbf{x})$ a function depending on the discretization method used for the pressure. When the row-sum of H is equal to one, the interpolation is consistent, which means that constant values are interpolated exactly.

The general opinion is that energy should be conserved over the interface leading to a conservative coupling approach⁸. The conservation properties depend both on the time and the spatial coupling used, which cannot be looked at separately if the system is solved in a partitioned way. However, in this paper we focus only on the spatial coupling. In the limit of very small time steps (virtual displacements, or steady state solution) or when a monolithic solution procedure is used with the same time integration method applied for both the flow and the structure, energy is globally conserved over the interface when

$$\int_{\Gamma_f} \mathbf{u}_f \cdot p_f \mathbf{n}_f ds = \int_{\Gamma_s} \mathbf{u}_s \cdot p_s \mathbf{n}_s ds, \quad (4)$$

with \mathbf{u} the displacement of the interface. This allows us to analyse the coupling in space separately.

Writing out the left hand side of (4) using (3) gives

$$\int_{\Gamma_f} \mathbf{u}_f \cdot p_f \mathbf{n}_f ds = \sum_{i=1}^{n_f^p} \left[\sum_{j=1}^{n_f^u} \int_{\Gamma_f} D_f^i N_f^j ds \mathbf{U}_{f_j} \right] \mathbf{P}_{f_i} = [M_{ff} \mathbf{U}_f]^T \mathbf{P}_f.$$

In a similar way we find for the right hand side of (4)

$$\int_{\Gamma_s} \mathbf{u}_s \cdot p_s \mathbf{n}_s ds = [M_{ss} \mathbf{U}_s]^T \mathbf{P}_s, \quad (5)$$

where matrices M_{ff} and M_{ss} are defined as follows

$$M_{ff}^{ij} = \int_{\Gamma_f} D_f^i N_f^j ds, \quad M_{ss}^{ij} = \int_{\Gamma_s} D_s^i N_s^j ds. \quad (6)$$

Energy is then globally conserved when

$$\begin{aligned} [M_{ff} \mathbf{U}_f]^T \mathbf{P}_f &= [M_{ss} \mathbf{U}_s]^T \mathbf{P}_s \quad \Rightarrow \quad \mathbf{U}_s^T H_{sf}^T M_{ff}^T \mathbf{P}_f = \mathbf{U}_s^T M_{ss}^T \mathbf{P}_s \quad \Rightarrow \\ H_{sf}^T M_{ff}^T \mathbf{P}_f &= M_{ss}^T \mathbf{P}_s \quad \Rightarrow \quad \mathbf{P}_s = [M_{ff} H_{sf} M_{ss}^{-1}]^T \mathbf{P}_f. \end{aligned} \quad (7)$$

So choosing

$$H_{fs} = [M_{ff} H_{sf} M_{ss}^{-1}]^T \quad (8)$$

for the transformation of pressure over the interface results in global conservation of energy over the interface.

To obtain a consistent interpolation, a constant displacement and constant pressure should be exactly interpolated over the interface (similar to the patch test criterion in Lagrange Multiplier methods). This means that in the conservative approach both the row-sum of H_{sf} and the row-sum of $H_{fs} = [M_{ff} H_{sf} M_{ss}^{-1}]^T$ should be equal to one. For a general transformation matrix H_{sf} this is not the case as we will see in the following section where different setups of the transformation matrices are outlined. The main question is whether global conservation of energy or a consistent interpolation is preferred in fluid-structure interaction computations.

3 COUPLING METHODS

In this section three different coupling techniques are outlined which are commonly found in literature to couple non-matching meshes in FSI computations. All methods create a transformation matrix H_{AB} to be able to transfer known values at the interface of mesh A to the interface of mesh B .

3.1 Nearest neighbour interpolation

Nearest neighbour interpolation (NN) is a very simple method of transferring data from mesh A to mesh B ¹. A search algorithm determines the point x_A in mesh A that is closest to a given point x_B in mesh B . The variable in x_B is then assigned to have the same value as in x_A . In this way the transformation matrix H_{AB} becomes a Boolean matrix, with a single one in each row which implies that the transformation is consistent.

However, when the conservative approach is used, the interpolation is not consistent for the pressure. This can be shown for a very simple example. The configuration consists of two structure points and three flow points and is depicted in Figure 2 resulting in the following transformation matrix for the displacements

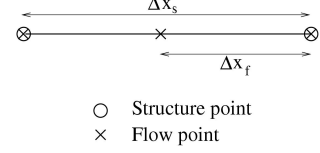


Figure 2: Simple 1D configuration.

$$H_{sf} = \begin{bmatrix} 1 & 0 \\ 1 & 0 \\ 0 & 1 \end{bmatrix}. \quad (9)$$

Constant basis functions are used in both the flow and the structure resulting in the following discretization matrices

$$M_f = \frac{1}{2} \begin{bmatrix} \Delta x_f & 0 & 0 \\ 0 & 2\Delta x_f & 0 \\ 0 & 0 & \Delta x_f \end{bmatrix}, \quad M_s = \frac{1}{2} \begin{bmatrix} \Delta x_s & 0 \\ 0 & \Delta x_s \end{bmatrix}. \quad (10)$$

The conservative transformation matrix for the pressure given in (8) then becomes

$$H_{fs} = \frac{\Delta x_f}{\Delta x_s} \begin{bmatrix} 1 & 2 & 0 \\ 0 & 0 & 1 \end{bmatrix}. \quad (11)$$

It can easily be seen that the row-sum of matrix H_{fs} is not equal to one, and the interpolation is therefore not consistent.

3.2 Weighted residual method

The method described in this section is based on the weak formulation of the conservation of loads or displacements over the interface^{2,3}. The starting point is the kinematic (1a) or dynamic boundary condition (1b) at the fluid-structure interface Γ in the continuous form

$$\mathbf{w}_B(\mathbf{x}) = \mathbf{w}_A(\mathbf{x}) \quad \text{on } \Gamma \quad \mathbf{w} = \{\mathbf{u}, p\mathbf{n}\}. \quad (12)$$

This equality can be approximately satisfied by a weighted residual method. Both sides are multiplied by a set of weighting functions ϕ_k and integrated over the fluid structure

interface resulting in

$$\int_{\Gamma} \phi_k(x) \mathbf{w}_B(\mathbf{x}) dx = \int_{\Gamma} \phi_k(x) \mathbf{w}_A(\mathbf{x}) dx. \quad (13)$$

Also the following approximation for the quantities is used

$$\mathbf{w}_B(x) = \sum_{i=1}^{n_B} N_B^i(x) \mathbf{W}_{B_i}, \quad \mathbf{w}_A(x) = \sum_{j=1}^{n_A} N_A^j(x) \mathbf{W}_{A_j}, \quad (14)$$

with $\mathbf{W}_{A,B}$ containing the values of $\mathbf{w}_{A,B}$ in the points on the interface of mesh A and B , respectively, $N_{A,B}$ the basis function of mesh A or B and $n_{A,B}$ the number of unknowns at the interface of mesh A or B . Together this yields

$$\int_{\Gamma} \phi_k(x) \sum_{i=1}^{n_B} N_B^i(x) \mathbf{W}_{B_i} dx = \int_{\Gamma} \phi_k(x) \sum_{j=1}^{n_A} N_A^j(x) \mathbf{W}_{A_j} dx. \quad (15)$$

For the displacement this is equal to the compatibility equation obtained by a Lagrange Multiplier method. When a Galerkin method is used there are two possibilities for ϕ , the basis function of the flow or the structure, so we can write

$$\sum_{i=1}^{n_B} \underbrace{\left[\int_{\Gamma} N_{\alpha}^k N_B^i dx \right]}_{C_{\alpha B}^{ki}} \mathbf{W}_{B_i} = \sum_{j=1}^{n_A} \underbrace{\left[\int_{\Gamma} N_{\alpha}^k N_A^j dx \right]}_{C_{\alpha A}^{kj}} \mathbf{W}_{A_j} \quad \text{for } k = 1, \dots, n_{\alpha}, \quad (16)$$

with $\alpha \in \{A, B\}$. This can be written in matrix form as

$$C_{\alpha B} \mathbf{W}_B = C_{\alpha A} \mathbf{W}_A, \quad (17)$$

with $C_{\alpha B}$ an $n_{\alpha} \times n_B$ matrix and $C_{\alpha A}$ an $n_{\alpha} \times n_A$ matrix.

Since we transfer data from mesh A to mesh B we need to solve for the side of mesh B , because the value of \mathbf{w} on mesh A is assumed to be known. This means that we have to choose $\alpha = B$ to be able to invert matrix $C_{\alpha B}$, so we obtain

$$\mathbf{W}_B = C_{BB}^{-1} C_{BA} \mathbf{W}_A. \quad (18)$$

As a consequence the transformation matrix is defined as $H_{AB} = C_{BB}^{-1} C_{BA}$.

Consistent approach To interpolate constant values exactly to obtain a consistent interpolation we need

$$C_{BB} \boldsymbol{\beta}_B = C_{BA} \boldsymbol{\beta}_A, \quad (19)$$

with $\beta_{A,B}$ a vector of length n_A or n_B respectively with constant value β . Using (16) this becomes

$$\sum_{i=1}^{n_B} \left[\int_{\Gamma} N_B^k N_B^i dx \right] \beta = \sum_{j=1}^{n_A} \left[\int_{\Gamma} N_B^k N_A^j dx \right] \beta \quad \text{for } k = 1, \dots, n_B. \quad (20)$$

Using the fact that

$$\sum_{k=1}^{n_{\alpha}} N_{\alpha}^k = 1 \quad \text{and} \quad \int_{\Gamma_{\alpha}} N_{\alpha}^k dx = 1, \quad (21)$$

we can derive for the left hand side

$$\sum_{i=1}^{n_B} \left[\int_{\Gamma} N_B^k N_B^i dx \right] \beta = \beta \int_{\Gamma} N_B^k \left[\sum_{i=1}^{n_B} N_B^i \right] dx = \beta \int_{\Gamma} N_B^k dx = \beta, \quad (22)$$

and for the right hand side

$$\sum_{j=1}^{n_A} \left[\int_{\Gamma} N_B^k N_A^j dx \right] \beta = \beta \int_{\Gamma} N_B^k \left[\sum_{j=1}^{n_A} N_A^j \right] dx = \beta \int_{\Gamma} N_B^k dx = \beta. \quad (23)$$

Therefore the transformation is consistent.

All that remains is the selection of the discrete interface over which the integrals are integrated in (16), because generally $\Gamma_A \neq \Gamma_B \neq \Gamma$. For the matrix C_{BB} it is most practical to integrate over Γ_B because both the values of N_B^k and N_B^i are known at that discretised interface. To obtain a consistent interpolation the integrals in matrix C_{BA} then also have to be integrated over Γ_B , otherwise (23) is unequal to (22).

Conservative approach We now investigate the consistency of the pressure when the conservative coupling approach is used. We start again with the discretized kinematic boundary condition (2a), where the weighted residual method gives us

$$H_{sf} = C_{ff}^{-1} C_{fs}. \quad (24)$$

Substituting this in (7) gives

$$\mathbf{P}_s = [M_{ff} C_{ff}^{-1} C_{fs} M_{ss}^{-1}]^T \mathbf{P}_f. \quad (25)$$

When the discretisation of the pressure and displacement in the flow are equal, so $N_f = D_f$ and $n_f^u = n_f^p$, then $M_{ff} = C_{ff}$ and (25) becomes

$$\mathbf{P}_s = [C_{fs} M_{ss}^{-1}]^T \mathbf{P}_f \quad \text{or} \quad M_{ss} \mathbf{P}_s = C_{sf} \mathbf{P}_f. \quad (26)$$

To be consistent we need

$$M_{ss} \boldsymbol{\beta}_s = C_{sf} \boldsymbol{\beta}_f, \quad (27)$$

with $\boldsymbol{\beta}_{s,f}$ a vector of length n_s or n_f respectively with constant value β . We can derive in a similar way as in (22) and (23) that this is equal to

$$\int_{\Gamma_s} N_s^k dx = \int_{\Gamma_f} N_s^k dx. \quad (28)$$

So only when the meshes are matching, $\Gamma_f = \Gamma_s$, equation (27) is satisfied and the method is both conservative and consistent for the pressure values.

Gauss integration For the evaluation of C_{BA} some kind of projection between the two meshes is needed, because N_A is only defined on mesh A . The integrals appearing in C_{BA} can be computed using Gauss integration (GI)^{2,4}. However, an overlay mesh has to be created to ensure that the basis functions on both sides of the discrete interface are continuous within a cell, to assure an exact evaluation of the integral. The overlay mesh is obtained by projecting the cells of mesh A on mesh B and taking the intersection of both meshes. This results in the following evaluation

$$C_{BA}^{kj} = \int_{\Gamma_B} N_B^k(x) N_A^j(x) dx \approx \sum_{i=1}^{n_{over}} \sum_{g=1}^{n_{gp,i}} w_g N_B^k(x_{g,i}) N_A^j(\Pi_A(x_{g,i})), \quad (29)$$

where n_{over} is the number of overlay cells, $n_{gp,i}$ is the number of Gauss quadrature points x_g in overlay cell i ; w_g the weight of the g^{th} quadrature point and $\Pi_A(x_{g,i})$ the projection of $x_{g,i}$ from mesh B on mesh A . The number of Gauss points to be used should be chosen equal to the underlying order of the discretisation. The Gauss points need to be orthogonally projected onto mesh B . This projection has to be accurate and take into account the normals of the used basis functions, otherwise the order of the total interpolation decreases.

3.3 Radial basis function interpolation (RBF)

The third class of coupling methods is based on the use of spline functions^{5,6,7}. The quantity to be transferred from mesh A to mesh B is approximated by a sum of basis functions both at the interface of mesh A and mesh B

$$\mathbf{w}_i(\mathbf{x}) = \sum_{j=1}^{n_A} \gamma_j \phi(\|\mathbf{x} - \mathbf{x}_{A_j}\|) + q(\mathbf{x}) \quad i = \{A, B\}, \quad \mathbf{w} = \{\mathbf{u}, p\} \quad (30)$$

where \mathbf{x}_{A_j} are the centres in which the values are known, in this case the nodes at the interface of mesh A , q a polynomial, and ϕ a given radial basis function with respect to the

Euclidean distance $||\mathbf{x}||$. Different suitable radial basis functions available in literature are presented in the next paragraph. The coefficients γ_j and the polynomial q are determined by the interpolation conditions

$$\mathbf{w}_A(\mathbf{x}_{A_j}) = \mathbf{W}_{A_j}, \quad (31)$$

with \mathbf{W}_A containing the discrete values of \mathbf{w}_A at the interface of mesh A , and the additional requirements

$$\sum_{j=1}^{n_A} \gamma_j s(\mathbf{x}_{A_j}) = 0, \quad (32)$$

for all polynomials s with a degree less than or equal to that of polynomial q . The minimal degree of polynomial q depends on the choice of the basis function ϕ . A unique interpolant is given if the basis function is a conditionally positive definite function. If the basis functions are conditionally positive definite of order $m \leq 2$, as is the case for the functions used in this paper, a linear polynomial can be used⁵. A consequence of using a linear polynomial is that constant values are exactly interpolated leading to a consistent interpolation.

For the known quantity at the interface of mesh A (30) and (32) can be written in matrix form as follows

$$\begin{bmatrix} \mathbf{W}_A \\ 0 \end{bmatrix} = \begin{bmatrix} \Phi_{AA} & Q_A \\ Q_A^T & 0 \end{bmatrix} \begin{bmatrix} \boldsymbol{\gamma} \\ \boldsymbol{\beta} \end{bmatrix}, \quad (33)$$

with $\boldsymbol{\gamma}$ containing the coefficients γ_j , $\boldsymbol{\beta}$ the coefficients of the linear polynomial q , Φ_{AA} an $n_A \times n_A$ matrix containing the evaluation of the basisfunction $\phi_{A_i A_j} = \phi(||\mathbf{x}_{A_i} - \mathbf{x}_{A_j}||)$ and Q_A a $n_A \times 4$ matrix with row j given by $[1 \ x_{A_j} \ y_{A_j} \ z_{A_j}]$.

For the unknown quantity at the interface of mesh B we can write in a similar notation

$$\mathbf{W}_B = [\Phi_{BA} \ Q_B] \begin{bmatrix} \boldsymbol{\gamma} \\ \boldsymbol{\beta} \end{bmatrix}. \quad (34)$$

Combining (33) and (34) gives the relation

$$\mathbf{W}_B = \underbrace{[\Phi_{AB} \ Q_B] \begin{bmatrix} \Phi_{AA} & Q_A \\ Q_A^T & 0 \end{bmatrix}^{-1}}_{\tilde{H}} \begin{bmatrix} \mathbf{W}_A \\ 0 \end{bmatrix} \quad (35)$$

and we can define the transformation matrix H_{AB} as the first n_B rows and n_A columns of matrix \tilde{H} to obtain $\mathbf{W}_B = H_{AB} \mathbf{W}_A$. In this way no orthogonal projection and search algorithm is needed, but the computation involves the inversion of a relatively small matrix. The number of rows and columns of this matrix is equal to the number of flow or structure points on the fluid-structure interface, which is usually very small compared to the total number of structure and flow points.

Radial basis functions Interpolation with RBF's has become a very powerful tool in multivariate approximation theory through scattered data, because of its excellent approximation properties¹¹. RBF's can be divided into two groups, functions with compact support and functions with global support. Beckert and Wendland⁵ use compact supported radial basis functions based on polynomials where a C^2 radial basis function gives the best result. This function is defined as

$$\phi(\|\mathbf{x}\|) = (1 - \|\mathbf{x}\|/r)_+^4 (4\|\mathbf{x}\|/r + 1), \quad (36)$$

where the subscript $+$ means that only positive values are taken into account and is in the remainder of the paper abbreviated by RBF. The radius r defines the support of the radial basis function. A large support radius yields a good approximation order, but then a full matrix system has to be solved. What is more, too large radii lead to singular matrices, because then all the entries of Φ_{AA} are approximately equal to one. A small support radius leads to a stable system with a band matrix that can be easily solved, but the interpolation is less accurate than with a large support radius. For an accurate computation the support radius for a fluid-structure interaction problem should be chosen at least as large as the maximum distance of all centres with their nearest neighbours in both meshes.

Several global radial basis functions have been tested and evaluated for analytical interpolation tests as well as real fluid-structure interaction computations by Smith et al^{6,7}. From this work the following two functions are shown to be the most robust, cost effective and accurate of the methods tested:

- Multi-quadric Biharmonic splines (MQ)

$$\phi(\|\mathbf{x}\|) = \sqrt{\|\mathbf{x}\|^2 + a^2}. \quad (37)$$

- Thin-plate splines (TPS)

$$\phi(\|\mathbf{x}\|) = \|\mathbf{x}\|^2 \log_{10} \|\mathbf{x}\|. \quad (38)$$

The MQ-method uses a parameter a that controls the shape of the basis functions. A large value of a gives a flat sheetlike function, while a small value of a gives a narrow conelike function. The value of a is typically chosen to be in the range $10^{-5} - 10^{-3}$. In this paper we use the value $a = 10^{-3}$. In contrast with the radial basis functions used by Beckert and Wendland, these two functions are defined on the entire domain. As a result, always a full matrix system has to be solved.

Because constant values are exactly recovered, the interpolation is consistent. However, when the conservative coupling approach is used, the interpolation is not consistent for the transformation of pressure values. The reason for this is similar to the one showed for nearest neighbour interpolation.

4 ANALYTICAL TEST PROBLEM

In this section the different coupling methods are compared for a smooth analytical problem, to be able to investigate their general interpolation properties separately. Both the consistent and conservative approach are applied for all the methods. The 'flow' and 'structure' points are located on the same analytical boundary in the form of a sine, $q_e = 0.2 \sin(2\pi x)$, with $x \in [-0.5, 0.5]$. The flow and structure interface are non-matching in the sense that they differ by the discretization of this common boundary. Both the number of flow and structure cells is varied. We use $n_f = 21 \cdot 2^k$ flow cells and $n_s = 7 \cdot 2^k$ structure cells, with $k \in \{0, 1, 2, 3, 4, 5\}$, leading to a ratio of 33%. A third order finite element method is used for the discretization. We will investigate both the error in the displacement of the flow boundary and the error in the pressure received by the structure obtained with the conservative and consistent approach.

Displacement of flow boundary In the structure points a displacement is assigned in the form of a cosine, $q = 0.01 \cos(2\pi x)$. The displacement in the flow points is then interpolated from the structure points, using one of the coupling methods, and compared with the exact values of the cosine. The L_2 -error of the displacement in the flow points versus the number of structure points after one interpolation step is depicted in Figure 3. It can be seen that NN is only first order accurate. The MQ and TPS method are second

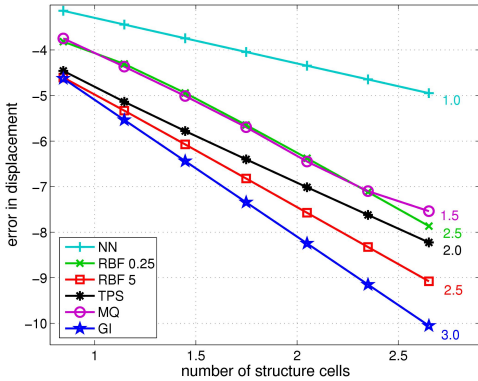


Figure 3: Error in displacement.

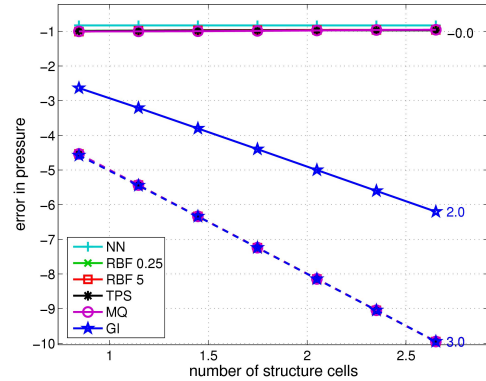


Figure 4: Error in pressure (—: conservative, ---: consistent).

order accurate where the accuracy of the TPS method is higher. The RBF method has an order of about 2.5, but the accuracy depends on the value of the radius: the larger the non-dimensional radius r , the more accurate the method. With $r = 5$, RBF is more accurate than TPS and with $r = 0.25$ it is comparable to MQ. The order of the GI method is the same as the order of the discretization. For a discretization order higher than two it is the most accurate method. In this paper we only show the results for a third order discretization.

Pressure received by structure Also a pressure in the form of a cosine, $p = 0.01 \cos(2\pi x)$, is assigned to the flow points and interpolated to the structure points either using the conservative or consistent approach. The L_2 -error of the pressure in the structure points versus the number of structure points after one interpolation step is depicted in Figure 4. The solid line is obtained with the conservative and the dotted line with the consistent approach. It can be seen that only the GI method converges when the conservative approach is used. The order of conservative GI is one lower than expected from the discretization order. When the consistent approach is used, for all methods the interpolation error is smaller than the discretization error leading to a third order convergence. This is due to the fact that the pressure is transferred from the finer flow grid to the coarser structure grid.

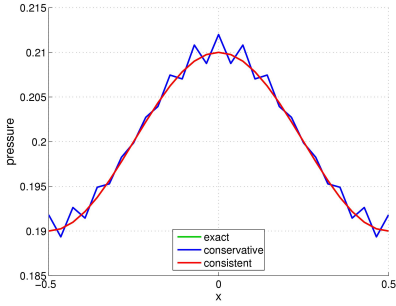


Figure 5: Pressure received by the structure obtained with the GI method for $n_f = 441$ and $n_s = 49$.

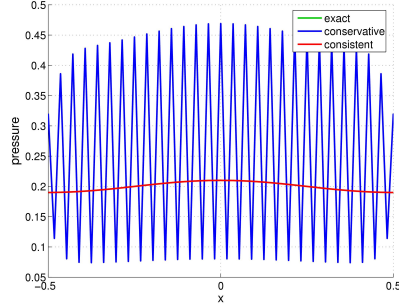


Figure 6: Pressure received by the structure obtained with the RBF method with $r = 5$ for $n_f = 441$ and $n_s = 49$.

The reason for the lower convergence for the conservative approach can be seen in Figures 5 and 6, where the exact pressure obtained by the structure and the ones obtained with the conservative and consistent approach are shown for the GI and RBF method with $r = 5$, respectively. The difference between the exact solution and the one obtained with the consistent approach is barely visible. However, the solution obtained with the conservative approach shows large oscillations. Except for the GI method, the amplitude of these wiggles does not reduce for finer meshes, leading to the zeroth order convergence.

In Figure 7 the difference in work between the flow and structure interface is depicted. When the conservative approach is used, this difference is zero, as expected. With the consistent approach the difference decreases with approximately one order higher than the order of the coupling method. So even as the consistent approach is not strictly globally conservative for the energy over the interface, the error decreases consistently.

Efficiency The efficiency is not the most important issue, because the computation time needed for the coupling is usually much smaller than, for example, the time needed for the flow solve. However, we want to investigate if the difference in efficiency between the methods is considerable. To obtain an estimation of the efficiency of the methods,

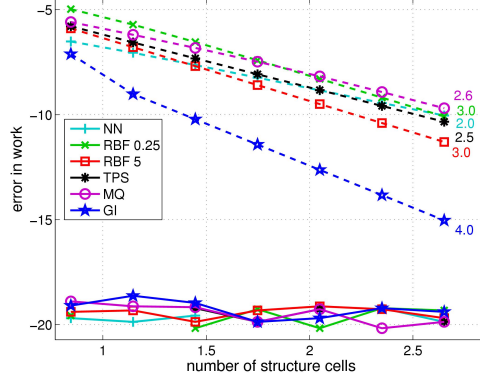


Figure 7: Difference in work of the different methods (—: conservative, ---: consistent).

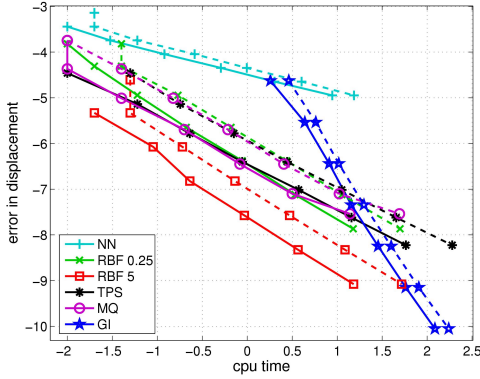


Figure 8: Efficiency of the displacement (—: conservative, ---: consistent).

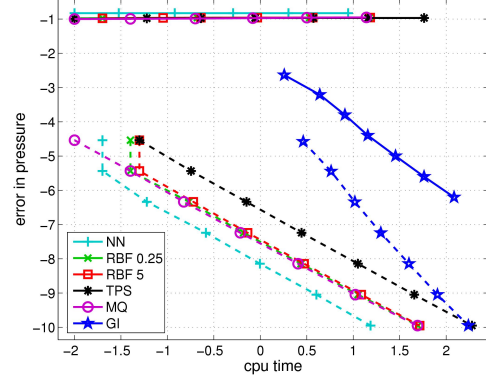


Figure 9: Efficiency of the pressure (—: conservative, ---: consistent).

the computation time needed to obtain a certain accuracy using Matlab version 7.0.1 on a 3 GHz computer is shown for the displacement and pressure in Figures 8 and 9, respectively. The closer the line is to the lower left corner, the more efficient the method. For the displacement the conservative approach is most efficient for all methods, where the highest efficiency is obtained with the RBF method with $r = 5$. The GI and NN method are the least efficient because they need a projection and search algorithm. For this test case a simple algorithm is used which performs a loop over the two closest elements in both directions. For the pressure the consistent approach is most efficient, because the conservative approach converges with a lower order (if it converges at all). This time NN is most efficient, closely followed by the radial basis function methods. The main conclusion is that the GI method, although it is more accurate for higher order discretizations, does need much more computation time than the methods based on radial basis function interpolation. The computational costs of the GI method also increase when a higher discretization order is used, because the projection algorithm becomes more complicated.

Also other analytic problems are investigated with different configurations of the displacement and pressure to be interpolated, different configurations of the interface and various ratios between flow and structure cells. The conclusions that can be drawn from the results of these test cases are similar to the ones described above. Overall it can be concluded that for this simple analytic problem the consistent approach is preferred over the conservative approach. NN is only first order accurate and therefore the least accurate method. When the discretization order of the total system is higher than two, the GI method is the best choice. However, its implementation is more difficult and the computation time is higher than for the RBF methods. Therefore, when the discretization of the total system is of order two or lower, or less important, the RBF methods are preferred where the RBF with $r = 5$ is the best choice.

5 QUASI-1D FSI PROBLEM

For the investigation of the behaviour of the methods in FSI simulations a quasi-1D problem is used. It is chosen such that it allows the investigation of the problems arising with non-matching meshes. We consider a quasi-1D channel with a flexible curved wall. The main velocity of the compressible flow is in the x -direction and the structure is modelled as a membrane. The diameter of the channel may vary due to a pressure difference between the pressure in the flow and the pressure in the wall. Considering only the static case allows to analyze the coupling in space separately, excluding errors based on time-coupling. To obtain the steady state solution an iterative approach is used. The existence of a numerical steady state solution is determined by computation of a numerically 'exact' solution on a very fine mesh by directly solving the steady state problem on matching meshes.

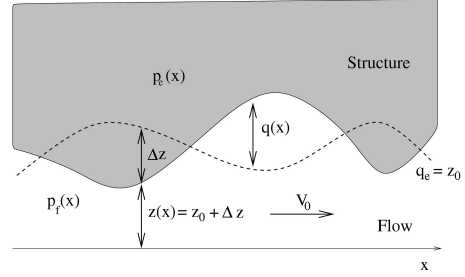


Figure 10: Configuration of the quasi-1D FSI problem.

5.1 Flow equations

A simple flow model is used which is valid for supersonic flow over a panel:

$$p_f = -\rho_0 c_0 V_0 \partial_x z, \quad (39)$$

with ρ_0 , c_0 and V_0 the density, speed of sound and velocity, respectively, assumed to be constant, p_f the pressure and $z = z_0 + \Delta z$ the location of the panel which is equal to the initial location of the panel, z_0 , plus the displacement from this initial position, Δz .

For convenience the variables are scaled as follows

$$\bar{x} = \frac{x}{L}, \quad \bar{V}_0 = \frac{V_0}{c_0}, \quad \bar{p}_f = \frac{p_f}{\rho_0 c_0^2}, \quad \bar{z} = \frac{z}{L}, \quad (40)$$

with L the length of the channel. This results in the following non-dimensional equation:

$$\bar{p}_f = -\bar{V}_0 \partial_x \bar{z}. \quad (41)$$

For notation purposes the bars are dropped in the remainder of the paper. To discretize the equations, a third order finite element discretization is used.

5.2 Structure equations

The equation that describes the behaviour of the flexible wall is given by

$$\kappa q - T \partial_{xx} q = p_s - p_e, \quad (42)$$

where q is the displacement from the 'dry' equilibrium position, $q_e(x)$, when $p_s = p_e$; p_s is the pressure acting on the wall, p_e is the pressure at the wall, assumed to be constant, κ the elasticity per unit length and T the longitudinal tension per unit length. Again the variables are scaled using the non-dimensional variables of (40) and the additional variables

$$\bar{q} = \frac{q}{L}, \quad \bar{p}_s = \frac{p_s}{\rho_0 c_0^2}, \quad \bar{p}_e = \frac{p_e}{\rho_0 c_0^2}, \quad \bar{\kappa} = \frac{\kappa L}{\rho_0 c_0^2}, \quad \bar{T} = \frac{T}{L \rho_0 c_0^2}. \quad (43)$$

This results in an equation which has two non-dimensional physical parameters $\bar{\kappa}$ and \bar{T} and has the same form as (42). In the remainder of the paper the bars are dropped. Again a third order finite element discretization is used to discretize the equations in space.

5.3 Coupling procedure

Coupling between the fluid and the structure equations is obtained through the dynamic (1a) and kinematic (1b) boundary conditions at the fluid-structure interface. A simple iterative coupling procedure is implemented to obtain the steady state solution. This iterative approach proceeds as follows

1. Calculate $\mathbf{p}_s = H_{fs} \mathbf{p}_f$.
2. Calculate the new displacement of the structure, \mathbf{q} from (42).
3. Obtain $\Delta \mathbf{z} = H_{sf} \mathbf{q}$ and update the location of the wall $\mathbf{z} = \mathbf{z}_0 + \Delta \mathbf{z}$.
4. Calculate \mathbf{p}_f from (41).

Repeat until the change in \mathbf{q} is smaller than a certain threshold. To obtain a numerically 'exact' solution the steady state problem is solved at once on very fine matching meshes. This is equivalent to solving the following equations on a fine mesh

$$\kappa q + V_0 \partial_x q - T \partial_{xx} q = -V_0 \partial_x q_e - p_e, \quad (44a)$$

$$p = -V_0 \partial_x q. \quad (44b)$$

For obtaining the 'exact' solution a fourth order finite element discretization is used to discretize the equations in space.

5.4 Results

For the test cases the following configuration is used. The boundaries of the domain are $x_{min} = -0.5$ and $x_{max} = 0.5$ and the initial shape of the tube wall is given by

$$z_0(x) = a_0 - a_1 e^{-a_2 x^2}, \quad (45)$$

where the parameters have the values $a_0 = 0.5$, $a_1 = 0.25$ and $a_2 = 80$. This means that we have a smooth converging/diverging channel. The 'dry' equilibrium position of the membrane, q_e , is equal to this initial shape. The values used for the non-dimensional structure parameters are: $\kappa = 50$ and $T = 0.04$, which results in a rather flexible membrane. For the flow velocity yields $V_0 = 3$, corresponding to a supersonic flow of Mach 3. Initially the pressure in the flow, \mathbf{p}_f , the pressure in the wall, \mathbf{p}_e , and the displacement \mathbf{q} are all equal to zero. We use $n_f = 21 \cdot 2^k$ flow cells and $n_s = 6 \cdot 2^k$ structure cells, with $k \in \{0, 1, 2, 3, 4, 5\}$, leading to a ratio of approximately 30%.

The L_2 -error of the displacement in the flow points versus the number of structure points is depicted in Figure 11. The solid line is obtained with the conservative and the dotted line with the consistent approach. The gray lines are added to indicate the discretization error and are generated with matching meshes: the solid gray line with $n_s = n_f = 21 \cdot 2^k$ and the dotted line with $n_f = n_s = 6 \cdot 2^k$. Above these lines the coupling error of a method is higher than the discretization error. NN is again the least

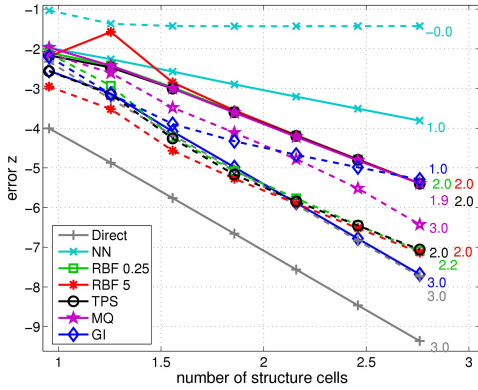


Figure 11: Error in displacement (—: conservative, — —: consistent).

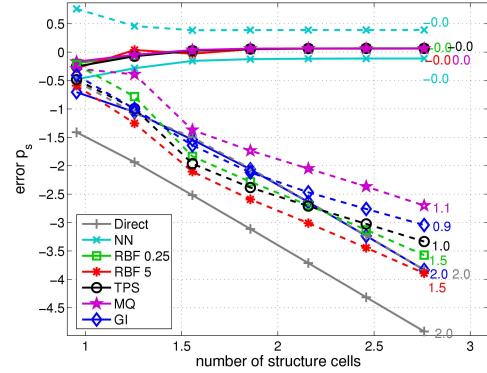


Figure 12: Error in pressure (—: conservative, — —: consistent).

accurate method. The methods based on radial basis function interpolation are second order accurate with the consistent approach giving the most accurate results where only for higher values of n_s the coupling error is higher than the third order discretization error. When the discretization error of the total system is second order or lower, the coupling error is always smaller than the discretization error. The coupling error for the GI method is always smaller than the discretization error for both the conservative and consistent approach.

The L_2 -error of the pressure in the structure points versus the number of structure points is depicted in Figure 4. Because the value for the pressure is obtained from the space derivative of z , the order of convergence should be one lower than for the displacement. It can be seen that the conservative approach leads again to a zeroth order error for all methods, except GI. The coupling error for the GI method is always smaller than the discretization error for both the conservative and consistent approach. The reduction in order for the conservative GI as can be seen in the analytical test case in Figure 4 is not visible, because of the order reduction caused by the space derivative.

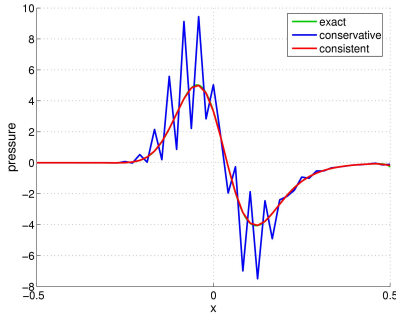


Figure 13: Pressure received by the structure obtained with the RBF method with $r = 5$ for $n_f = 441$ and $n_s = 36$.

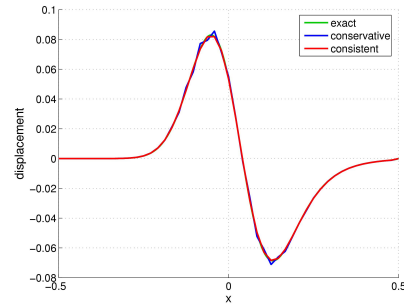


Figure 14: Displacement obtained with the RBF method with $r = 5$ for $n_f = 441$ and $n_s = 36$.

In Figures 13 and 14, the exact solution obtained by the structure and the ones obtained with the conservative and consistent approach for the RBF method with $r = 5$ are shown for the pressure obtained by the structure, p_s , and the displacement q , respectively. It can be seen that the large oscillations felt by the structure also result in small deviations in the displacement. The more flexible the structure, the larger these deviations become.

For this simple test problem, the computation time needed by the coupling algorithm is still considerable compared to the overall computation time. From Figures 15 and 16 it can be seen that the consistent RBF method with a large radius is the most efficient. The GI method is again the least efficient, because of the projection algorithm. The results for the difference in work are similar to the ones obtained by the analytical test case.

The main conclusion is that the NN method is not suitable for the coupling of non-matching meshes, because it is only first order accurate. The conservative approach should be used with the GI method, because it gives the highest accuracy and efficiency. However, the methods based on radial basis function interpolation show large oscillations in the pressure obtained by the structure, when the conservative approach is used. For these coupling methods the consistent approach provides the best accuracy and efficiency.

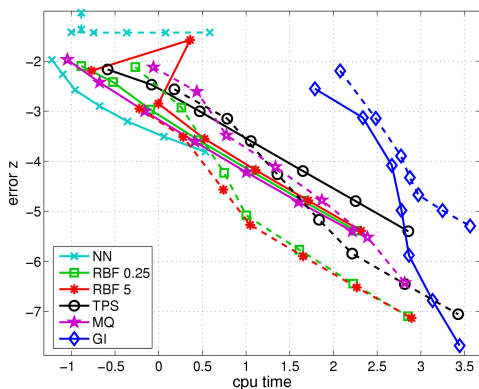


Figure 15: Efficiency for the displacement (—: conservative, ---: consistent).

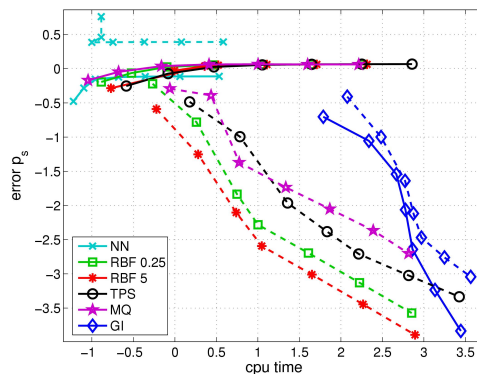


Figure 16: Efficiency for the pressure (—: conservative, ---: consistent).

6 CONCLUSIONS

In this paper we investigate the difference in accuracy and efficiency between the conservative and consistent approach for different coupling methods. The performance is investigated for an analytical test problem as well as a simple quasi-1D FSI problem. When the coupling method is based on a weighted residual formulation of the coupling conditions, the highest accuracy and efficiency are obtained with the conservative approach. For other coupling methods the conservative approach results in unphysical oscillations in the pressure received by the structure. When the structure is flexible enough these oscillations can result in deviations in the displacement. For these methods the consistent approach provides the best accuracy and efficiency.

Overall, when the discretization order of the total system higher than two, the conservative GI method is the best choice.. However, its implementation is more difficult and the computation time is higher than for the methods based on radial basis function interpolation. This is because the higher order of the GI method is only obtained when all the projection steps are accurately performed. Therefore, when the discretization of the total system is of order two or lower, or less important, the methods based on radial basis function interpolation are preferred where the compact RBF with a high support radius is the best choice.

Up to now only a simple steady quasi-1D fluid-structure interaction problem has been considered. Future research will focus on the investigation of time-dependent and more realistic multi-dimensional problems by coupling existing fluid and structure solvers.

REFERENCES

- [1] P. Thévenaz, T. Blu, and M. Unser, Interpolation revisited, *IEEE T. Med. Imag.*, Vol. **19**, No. 7, 739–758, (2000).
- [2] J.R. Cebal and R. Löhner, Conservative load projection and tracking for fluid-

- structure problems, *AIAA J.*, Vol. **35**, No. 4, 687–692, (1997).
- [3] R. Löhner, C. Yang, J. Cebal, J.D. Baum, H. Luo, D. Pelessone and C.Charman, Fluid-structure interaction using a loose coupling algorithm and adaptive unstructured grids, in M. Hafez and K. Oshima (eds.), *Computational fluid dynamics review*, John Wiley, (1995).
 - [4] N. Maman and C. Farhat, Matching fluid and structure meshes for aeroelastic computations: a parallel approach, *Comp. Stru.*, Vol. **54**, No. 4, 779–785, (1995).
 - [5] A. Beckert and H. Wendland. Multivariate interpolation for fluid-structure-interaction problems using radial basis functions. *Aerosp. Sci. Technol.*, Vol. **0**, 1–11, (2001).
 - [6] M.J. Smith, C.E.S. Cesnik and D.H. Hodges, Evaluation of some data transfer algorithms for noncontiguous meshes, *J. Aerospace Eng.*, Vol. **13**, No. 2, 52–58, (2000a).
 - [7] M.J. Smith, D.H. Hodges and C.E.S. Cesnik, Evaluation of computational algorithms suitable for fluid-structure interaction, *J. Airc.*, Vol. **37**, No. 2, 282–294, (2000b).
 - [8] C. Farhat, M. Lesoinne and P. le Tallec. Load and motion transfer algorithms for fluid/structure interaction problems with non-matching discrete interfaces: momentum and energy conservation, optimal discretization and application to aeroelasticity. *Comput. Methods Appl. Mech. Engrg.*, Vol. **157**, 95–114, (1998).
 - [9] R. Ahrem, A. Beckert and H. Wendland, A new multivariate interpolation method for large-scale coupling problems in aeroelasticity, Conference proceedings IFADS, Munich, (2005).
 - [10] A. de Boer, A.H. van Zuijlen and H. Bijl, Review of coupling methods for non-matching meshes, *Comput. Methods Appl. Mech. Engrg.*, accepted for publication, (2006).
 - [11] M. Buhmann, Radial basis functions, *Acta Numerica*, Vol. **9**, 1–38, (2000).
 - [12] *MpCCI, mesh-based parallel code coupling interface - Specification of MpCCI version 2.0*, Fraunhofer Institut for Algorithms and Scientific Computing SCAI, (2003).